DOI: 10.1021/ic101646p

Inorganic Chemistry
Article

Mixed-Valence Dinitrogen-Bridged Fe(0)/Fe(II) Complex

Leslie D. Field,*,† Ruth W. Guest,†,‡ and Peter Turner‡

†*School of Chemistry, The University of New South Wales, NSW 2052, Australia, and*
‡*School of Chemistry, University of Sydney, NSW 2006, Australia*

Received August 13, 2010

The reactions of a dinitrogen-bridged Fe(II)/Fe(II) complex $[(FeH(PP_3))_2(\mu\text{-}N_2)]^{2+}$ (**3**) ($PP_3 = P(CH_2CH_2PMe_2)_3$) with base were investigated using ^{15}N labeling techniques to enhance characterization. In the presence of base, **3** is initially deprotonated to the Fe(II)/Fe(0) dinitrogen-bridged complex $[(FeH(PP_3))(\mu\text{-}N_2)(Fe(PP_3))]^{+}$ (**4**) and then to the symmetrical Fe(0)/Fe(0) dinitrogen-bridged complex $(Fe(PP_3))_2(\mu\text{-}N_2)$ (**5**). $[(FeH(PP_3))(\mu\text{-}N_2)(Fe(PP_3))]^{+}$ (**4**) exhibits unusual long-range $^{31}P-^{31}P$ NMR coupling through the bridging dinitrogen ligand from the phosphines at the Fe(0) center and those at the Fe(II) center. Reaction of **4** with base under an atmosphere of argon resulted in the known dinitrogen Fe(0) complex $Fe(N_2)(PP_3)$ (**6**) and a solvent C−H activation product. Complexes **3**, **4**, and **5** were fully characterized by multinuclear NMR spectroscopy, and complexes **3** and **4** by X-ray crystallography.

Introduction

Investigations into the synthesis and reactions of dinitrogen complexes have been ongoing since the discovery of the first dinitrogen complex $[Ru(NH_3)_5(N_2)]^{2+}$ in 1965.[1] Dinitrogen can coordinate to metal centers via several modes, the most common of which is end-on binding.[2] In this mode, the formation of dinitrogen-bridged dinuclear complexes is relatively common because the donation of electron density from the metal center into the π^*-orbitals of the dinitrogen ligand renders the terminal N more nucleophilic. Several groups believe that iron is at the active site of nitrogenase,[3] while in work on the mechanism of molybdenum nitrogenases, Durrant[4] has proposed a mechanism involving a bimetallic center. In this mechanism, N_2 initially binds at the Mo center and requires the assistance of the Fe center for the reduction and eventual release of NH_3.

In 1975, Chatt et al.[5] achieved the first protonation of a dinitrogen complex to give ammonia by reacting *cis*-$W(N_2)_2(PMe_2Ph)_4$ with sulfuric acid in methanol. There are now many examples of reactions of dinitrogen complexes giving rise to the reduction products hydrazine and ammonia.[4,6−10] In 1995, dinitrogen triple bond cleavage, at a bridged dinuclear complex, was demonstrated by Laplaza and Cummins.[11,12] In a reaction ostensibly the reverse of dinitrogen triple bond cleavage, the bimolecular condensation of an Fe(IV) nitride to give an Fe(I) dinitrogen-bridged dimer was reported in 2004 by Betley and Peters.[13]

In this paper, we have turned our attention to the chemistry of a previously reported dinitrogen-bridged iron(II) hydride complex $[(FeH(PP_3))_2(\mu\text{-}N_2)]^{2+}$ (**3**) ($PP_3 = P(CH_2CH_2PMe_2)_3$).[14] We present the results of treatment of **3** with base, and subsequently with acid. The stepwise deprotonation of **3** to give a mixed valence iron(II)−iron(0) dinuclear species, $[(FeH(PP_3))(\mu\text{-}N_2)(Fe(PP_3))]^{+}$ (**4**), and then an iron(0)−iron(0) dimer, $(Fe(PP_3))_2(\mu\text{-}N_2)$ (**5**), is reported. Characterization of the unusual mixed valence dinuclear

*To whom correspondence should be addressed. E-mail: l.field@unsw.edu.au. Fax: +61 2 9385 8008. Phone: +61 2 9385 2700.

(1) Allen, A. D.; Senoff, C. W. *Chem. Commun.* **1965**, 621–2.
(2) Fryzuk, M. D.; Johnson, S. A. *Coord. Chem. Rev.* **2000**, *200−202*, 379–409.
(3) (a) Demadis, K. D.; Malinak, S. M.; Coucouvanis, D. *Inorg. Chem.* **1996**, *35*, 4038–4046. (b) Hughes, D. L.; Ibrahim, S. K.; Pickett, C. J.; Querne, G.; Laouenan, A.; Talarmin, J.; Queiros, A.; Fonseca, A. *Polyhedron* **1994**, *13*, 3341–3348. (c) Zhong, S. J.; Liu, C. W. *Polyhedron* **1997**, *16*, 653–661. (d) Deng, H. B.; Hoffmann, R. *Angew. Chem., Int. Ed. Engl.* **1993**, *32*, 1062–1065. Hidai, M. *Coord. Chem. Rev.* **1999**, *185−186*, 99. (e) Gambarotta, S.; Scott, J. *Angew. Chem., Int. Ed.* **2004**, *43*, 5298. (f) Schrock, R. R. *Acc. Chem. Res.* **2005**, *38*, 955. (g) Holland, P. L. *Can. J. Chem.* **2005**, *83*, 296. (h) Chirik, P. J. *Dalton Trans.* **2007**, 16. (i) Ohki, Y.; Fryzuk, M. D. *Angew. Chem., Int. Ed.* **2007**, *46*, 3180. (j) Forni, L. *Chim. Ind.* **2009**, *91*, 108. (k) Dance, I. G. *J. Am. Chem. Soc.* **2007**, *129*, 1076–1088. (l) Dance, I. G. *Dalton Trans.* **2008**, 5977–5991. (m) Dance, I. G. *Dalton Trans.* **2008**, 5992–5998.
(4) Durrant, M. C. *Biochemistry* **2002**, *41*, 13934–13945.
(5) Chatt, J.; Pearman, A. J.; Richards, R. L. *Nature* **1975**, *253*, 39–40.
(6) Hidai, M. *Coord. Chem. Rev.* **1999**, *185−186*, 99–108.
(7) Chirik, P. J. *Dalton Trans.* **2007**, 16–25.
(8) Yandulov, D. V.; Schrock, R. R. *Science* **2003**, *301*, 76–78.
(9) MacKay, B. A.; Fryzuk, M. D. *Chem. Rev.* **2004**, *104*, 385–401.
(10) Crossland, J. L.; Tyler, D. R. *Coord. Chem. Rev.* **2010**, *254*, 1883−1894.
(11) Laplaza, C. E.; Cummins, C. C. *Science* **1995**, *268*, 861–863.
(12) Laplaza, C. E.; Johnson, M. J. A.; Peters, J.; Odom, A. L.; Kim, E.; Cummins, C. C.; George, G. N.; Pickering, I. J. *J. Am. Chem. Soc.* **1996**, *118*, 8623–8638.
(13) Betley, T. A.; Peters, J. C. *J. Am. Chem. Soc.* **2004**, *126*, 6252–6254.
(14) Field, L. D.; Messerle, B. A.; Smernik, R. J. *Inorg. Chem.* **1997**, *36*, 5984–5990.

 Published on Web 09/03/2010

Scheme 1

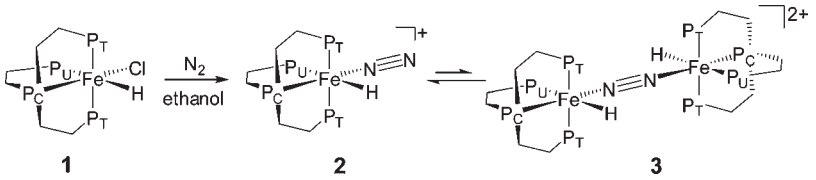

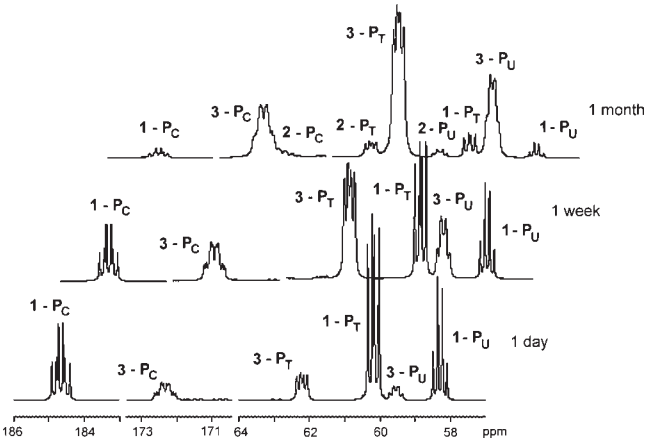

Figure 1. $^{31}P\{^1H\}$ NMR spectra showing the generation of $^{15}N_2$**-3** and $[Fe(^{15}N_2)H(PP_3)]^+$ $^{15}N_2$**-2** with the addition of $^{15}N_2$ over time to an ethanol/benzene-d_6 solution of $FeClH(PP_3)$ (**1**).

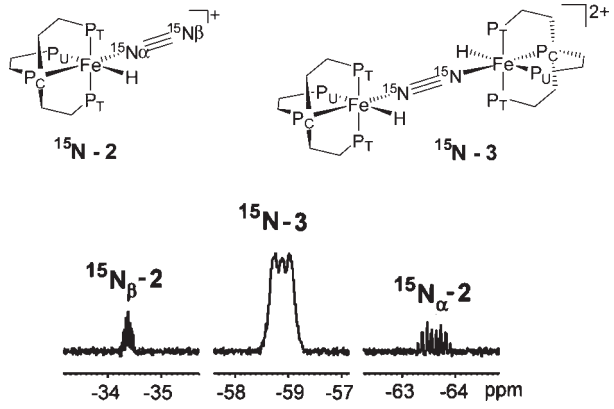

Figure 2. Resolution enhanced $^{15}N\{^1H\}$ NMR resonances of $[Fe(^{15}N_2)H(PP_3)]^+$ $^{15}N_2$**-2** and $[(FeH(PP_3))_2(\mu\text{-}^{15}N_2)]^{2+}$ $^{15}N_2$**-3** in ethanol/benzene-d_6.

complex **4** includes its analysis by X-ray crystallography and the observation of an unusual long-range $^5J_{P-P}$ coupling in the $^{31}P\{^1H\}$ NMR spectrum across the bridging dinitrogen.

Results and Discussion

The dinitrogen-bridged iron(II) hydride complex $[(FeH(PP_3))_2(\mu\text{-}N_2)]^{2+}$ (**3**) ($PP_3 = P(CH_2CH_2PMe_2)_3$) and its monomeric precursor $[Fe(N_2)H(PP_3)]^+$ (**2**) were synthesized by dissolution of $FeClH(PP_3)$ (**1**)[15] in ethanol under an atmosphere of N_2 as previously reported[14] (Scheme 1).

The ^{15}N labeled analogues of **2** and **3** were synthesized on an NMR scale by dissolution of $FeClH(PP_3)$ (**1**) in nitrogen-free ethanol, to which ^{15}N labeled dinitrogen, at a pressure of less than 1 atm, was added. Initially this led to a single resonance at δ −58.7 ppm in the ^{15}N NMR spectrum, and this corresponds to the symmetrical nitrogen-bridged species $^{15}N_2$**-3**.

The $^{31}P\{^1H\}$ NMR spectrum (Figure 1) shows the appearance of the three resonances of $^{15}N_2$**-3** with an additional 11 Hz $^3J_{P-N}$ coupling clearly apparent in the splitting of the ligand's central phosphorus P_C. There is no $^{15}N_2$ peak present in the ^{15}N NMR spectrum and no resonances which might correspond to dinitrogen species $^{15}N_2$**-2**. This result is in contrast to previous work,[14] which has shown that at higher pressures of dinitrogen (greater than 1 atm) the monometallic species **2** is initially the dominant species. The driving force under the conditions here is likely to be the preference for the $[FeH(PP_3)]^+$ moiety to coordinate a dinitrogen (bridged or otherwise) over an ethoxide or chloride in ethanol. Where there is a large excess of $FeClH(PP_3)$ (**1**), all the dinitrogen is complexed in the form of the nitrogen bridged species **3**. Further addition of $^{15}N_2$, over the course of several days, resulted in an increase in intensity of resonances for $^{15}N_2$**-3**, and the appearance of signals for $^{15}N_2$**-2** in both the $^{31}P\{^1H\}$ and ^{15}N NMR spectra as well as free $^{15}N_2$ at δ −71.6 ppm in the ^{15}N NMR spectrum. It was not possible to introduce sufficient labeled dinitrogen to the sample to completely convert the chlorohydride to either dinitrogen species.

A resolution enhanced $^{15}N\{^1H\}$ NMR spectrum (Figure 2) shows the resonances of the two dinitrogen containing species $^{15}N_2$**-2** and $^{15}N_2$**-3**. The monometallic species $^{15}N_2$**-2** has two resonances at δ −34.4 and −63.6 ppm assigned to N_β and N_α, respectively. This assignment is based on the presence of a larger $^{31}P-^{15}N$ coupling of N_α and its relatively high field chemical shift with respect to N_β.[16] $^{15}N_2$**-2·[BPh$_4$]** has been prepared previously by exchange of ^{15}N labeled dinitrogen with dinitrogen of unlabeled **2·[BPh$_4$]** in tetrahydrofuran (THF).[17] Because of its symmetry, the bridged species $^{15}N_2$**-3** exhibits only a single resonance at δ −58.9 ppm. The ^{15}N chemical shifts of $^{15}N_2$**-2** are typical for mononuclear iron-phosphine dinitrogen complexes.[17]

Diffraction quality crystals of ^{15}**N-3** as its tetra(3,5-bis(trifluoromethyl)phenyl)borate $[BAr^F{}_4]^-$ salt were grown by addition of sodium tetra(3,5-bis(trifluoromethyl)phenyl)borate to an ethanol solution of $^{15}N_2$**-3** and $^{15}N_2$**-2**. The solution was left under an atmosphere of argon for several weeks during which time, pale orange crystals of $^{15}N_2$**-3** deposited from the solution. The crystal structure of $^{15}N_2$**-3·[BAr$^F{}_4$]$_2$** has a center of symmetry about the N−N triple bond and contains slight disorder within the PP_3 ligand and the counteranion (Figure 3). Selected bond lengths and angles are presented in Table 1.

The four phosphorus atoms of the PP_3 ligand and the dinitrogen and hydride ligands of ^{15}**N-3·[BAr$^F{}_4$]$_2$** are arranged around the iron(II) centers in distorted octahedra. The Fe−P bond lengths are comparable with those of other iron

(15) Field, L. D.; Messerle, B. A.; Smernik, R. J.; Hambley, T. W.; Turner, P. *Inorg. Chem.* **1997**, *36*, 2884–2892.

(16) Donovan-Mtunzi, S.; Richards, R. L.; Mason, J. *J. Chem. Soc., Dalton Trans.* **1984**, 469–474.

(17) Field, L. D.; Hazari, N.; Li, H. L.; Luck, I. J. *Magn. Reson. Chem.* **2003**, *41*, 709–713.

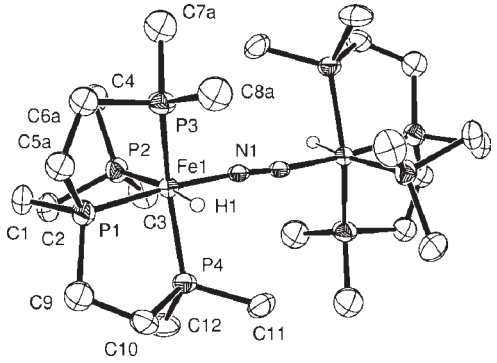

Figure 3. ORTEP plot (50% thermal ellipsoids, non-hydrogen atoms) of the complex cation of $^{15}N_2$-**3**·[BAr^F_4]$_2$. Atoms of 30% occupancy and selected hydrogen atoms have been excluded for clarity.

Table 1. Selected Bond Distances (Å) and Angles (deg) for [(FeH(PP_3))$_2$(μ-N_2)]-[BAr^F_4]$_2$ (**3**·[BAr^F_4]$_2$)

Bond Distances (Å)			
Fe(1)−N(1)	1.858(2)	Fe(1)−H(1)	1.45(2)
Fe(1)−P(1)	2.1628(11)	Fe(1)−P(2)	2.2276(10)
Fe(1)−P(3)	2.2249(10)	Fe(1)−P(4)	2.1983(10)
N(1)−N(1)	1.129(4)		
Bond Angles (deg)			
Fe(1)−N(1)−N(1)	174.7(3)	N(1)−Fe(1)−P(1)	175.22(7)
P(2)−Fe(1)−P(1)	85.94(4)	P(3)−Fe(1)−P(1)	85.03(4)
P(4)−Fe(1)−P(1)	84.49(4)	N(1)−Fe(1)−P(2)	94.78(7)
P(3)−Fe(1)−P(2)	105.20(4)	P(4)−Fe(1)−P(2)	104.26(4)
N(1)−Fe(1)−P(3)	99.31(7)	P(4)−Fe(1)−P(3)	147.86(3)
N(1)−Fe(1)−P(4)	90.76(7)	N(1)−Fe(1)−H(1)	92.3(11)
P(1)−Fe(1)−H(1)	86.9(11)	P(2)−Fe(1)−H(1)	172.9(11)
P(3)−Fe(1)−H(1)	74.4(11)	P(4)−Fe(1)−H(1)	74.8(11)

complexes of the PP_3 ligand [Fe(η^3-PhC≡C−C═C(H)Ph)-(PP_3)][BPh_4],[18] [FeCl(PPh_3)(PP_3)][BPh_4],[15] and [Fe(CO)(CH_3)-(PP_3)]Cl.[19] The P_T−Fe-P_T angles of these complexes are significantly greater than that of ^{15}**N-3**·[BAr^F_4]$_2$ most probably reflecting the smaller size of the hydride ligand of ^{15}**N-3** which provides less steric compression of the PP_3 ligand set. The N−N bond length of ^{15}**N-3** at 1.129(4) Å indicates a small degree of activation of the dinitrogen triple bond compared to free dinitrogen (1.0975 Å)[20] and is slightly longer than those of similar iron(II) dinitrogen hydride complexes [FeH(N_2)-(NP^{Ph}_3)][BPh_4] (NP^{Ph}_3 = N($CH_2CH_2PPh_2$)$_3$)[21] and [FeH(N_2)-(NP^{iPr}_3)][PF_6] (NP^{iPr}_3 = N($CH_2CH_2P^iPr_2$)$_3$)[22] at 1.10(1) and 1.113(4) Å, respectively. Dinitrogen-bridged iron complexes [Fe($PhBP^{iPr}_3$)]$_2$(μ-N_2)[15] ($PhBP^{iPr}_3$ = PhB($CH_2P^iPr_2$)$_3$), [Na($THF)_6$][(Fe($PhBP^{iPr}_3$))$_2$(μ-N_2)],[23] (LFe)$_2$(μ-N_2) (L = HC[C(^{t}Bu)N(2,6-^{i}Pr$_2$C$_6$H$_3$)]$_2$), K$_2$[(LFe)$_2$(μ-N_2)], Na$_2$[(LFe)$_2$-(μ-N_2)],[24] [Fe(CO)$_2$(PEt_3)$_2$]$_2$(μ-N_2),[25] and [Fe(CO)$_2$(P(O-CH_3)$_3$)$_2$]$_2$(μ-N_2)[26] have comparable N−N bond lengths to **3**·[BAr^F_4]$_2$ excepting the iron(0)−iron(I) dimer [Na-($THF)_6$][(Fe($PhBP^{iPr}_3$))$_2$(μ-N_2)] and the β-diketiminate complexes (LFe)$_2$(μ-N_2), K$_2$[(LFe)$_2$(μ-N_2)] and Na$_2$[(LFe)$_2$-(μ-N_2)] where the reported N−N bond lengths of 1.171(4), 1.182(5), 1.233(6), and 1.239(4) Å are slightly longer.

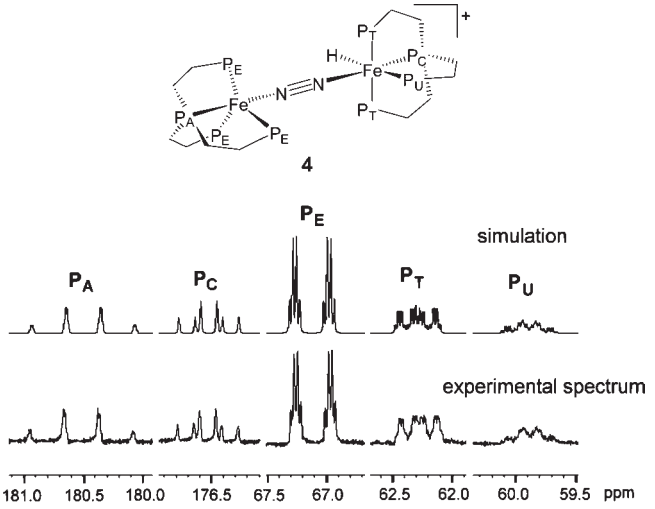

Figure 4. Resolution enhanced experimental spectrum and simulated $^{31}P\{^1H\}$ NMR (162 MHz) spectrum of [(FeH(PP_3))(μ-N_2)(Fe(PP_3))]-[BPh_4] (**4**·[BPh_4]) in THF-d_8.

Scheme 2

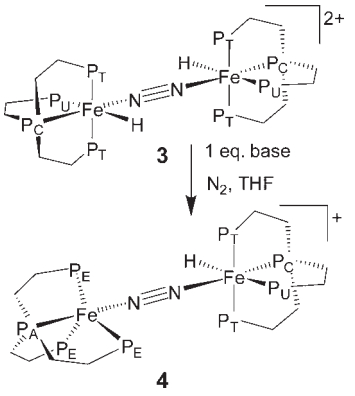

Treatment of [(FeH(PP_3))$_2$(μ-N_2)][BPh_4]$_2$ 3·[BPh_4]$_2$ with Base. The tetraphenylborate salt of **3** was isolated following literature procedures.[14] Treatment of a suspension of **3**·[BPh_4]$_2$ in THF with 1 equiv of base (potassium *t*-butoxide or potassium bis(trimethylsilyl)amide) and gentle heating (approximately 50 °C for 2 h) under dinitrogen results in the appearance of a red solution of [(FeH-(PP_3))(μ-N_2)(Fe(PP_3))][BPh_4] (**4**·[BPh_4]) (Scheme 2).

The $^{31}P\{^1H\}$ NMR spectrum of **4**·[BPh_4], shown in Figure 4, has five resonances at δ 180.7, 176.7, 67.0, 62.0, and 59.6 ppm in the ratio 1:1:3:2:1. These resonances are assigned to the apical phosphorus, P_A (180.7 ppm), and three equivalent terminal phosphorus atoms, P_E (67.0 ppm), of a trigonal bipyramidal iron(0) center and the four

(18) Field, L. D.; Messerle, B. A.; Smernik, R. J.; Hambley, T. W.; Turner, P. *J. Chem. Soc., Dalton Trans.* **1999**, 2557–2562.
(19) Field, L. D.; Li, H. L.; Messerle, B. A.; Smernik, R. J.; Turner, P. *J. Chem. Soc., Dalton Trans.* **2004**, 1418–1423.
(20) Sutton, L. E. *Tables of Interatomic Distances and Configuration in Molecules and Ions*; The Chemical Society: London, 1958.
(21) George, T. A.; Rose, D. J.; Chang, Y.; Chen, Q.; Zubieta, J. *Inorg. Chem.* **1995**, *34*, 1295–1298.
(22) MacBeth, C. E.; Harkins, S. B.; Peters, J. C. *Can. J. Chem.* **2005**, *83*, 332–340.
(23) Betley, T. A.; Peters, J. C. *J. Am. Chem. Soc.* **2003**, *125*, 10782–10783.
(24) Smith, J. M.; Lachicotte, R. J.; Pittard, K. A.; Cundari, T. R.; Lukat-Rodgers, G.; Rodgers, K. R.; Holland, P. L. *J. Am. Chem. Soc.* **2001**, *123*, 9222–9223.
(25) Kandler, H.; Gauss, C.; Bidell, W.; Rosenberger, S.; Buergi, T.; Eremenko, I. L.; Veghini, D.; Orama, O.; Burger, P.; Berke, H. *Chem.—Eur. J.* **1995**, *1*, 541–548.
(26) Berke, H.; Bankhardt, W.; Huttner, G.; Von Seyerl, J.; Zsolnai, L. *Chem. Ber.* **1981**, *114*, 2754–2768.

Table 2. Coupling Constants (Hz) Used in Simulation of $^{31}P\{^1H\}$ NMR (162 MHz) Spectrum of $[(FeH(PP_3))(\mu\text{-}N_2)(Fe(PP_3))][BPh_4]$ (**4·[BPh$_4$]**)

	P_A	P_E	P_C	P_T	P_U
P_A		46.7	0.85	2.0	2.2
P_E	46.7		0.90	4.5	5.3
P_C	0.85	0.90		29.7	22.0
P_T	2.0	4.5	29.7		18.0
P_U	2.2	5.3	22.0	18.0	

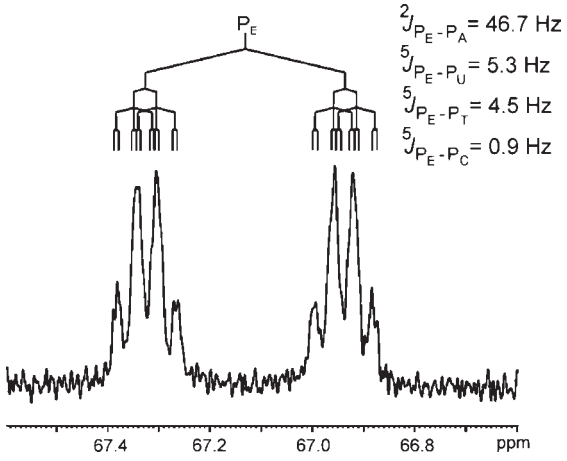

Figure 5. Splitting pattern of the P_E resonance of **4·[BPh$_4$]** in the $^{31}P\{^1H\}$ NMR spectrum showing the short- and long- range $^{31}P-^{31}P$ coupling.

phosphorus atoms, P_C (176.7 ppm), P_T (62.0 ppm), and P_U (59.6 ppm), of an octahedral iron(II) center. The chemical shifts of the terminal phosphorus atoms P_T and P_U are comparable to those of **3·[BPh$_4$]$_2$** while that of the central phosphorus P_C is 4 ppm downfield relative to **3·[BPh$_4$]$_2$**. It is clear from the $^{31}P\{^1H\}$ NMR spectrum, which is resolution enhanced and expanded in Figure 4, that there are small couplings (< 6 Hz) between all of the phosphorus atoms on the Fe(0) center and those on the Fe(II) center through the bridging N_2. A simulation of the spectra was achieved using the coupling constants given in Table 2, and its fit with the actual spectrum is illustrated in Figure 4. The splitting pattern of the terminal phosphorus P_E is illustrated in Figure 5.

The larger $^2J_{P-P}$ coupling constants across the trigonal bipyramidal iron site are consistent with an iron(0) center.[14,27] As might be expected, given the similarities in structure, coupling constants across the octahedral iron(II) center are very similar to those observed in the symmetrical dinuclear species $[(FeH(PP_3))_2(\mu\text{-}N_2)]^{2+}$ **3·[BPh$_4$]$_2$**. To our knowledge, no previous examples of long-range NMR coupling through a N−N triple bond exist in the literature. The $^5J_{P-P}$ coupling constants presented in Table 2, that is, those between P_E or P_A on the Fe(0) center and P_U, P_C or P_T on the Fe(II) center, are of the same order of magnitude as those reported across a phosphine substituted aromatic ring.[28] The high field region of the ^1H NMR spectrum has a multiplet at δ −12.5 ppm which has a splitting pattern very similar to that of **3·[BPh$_4$]$_2$**.

The ^{15}N labeled analogue of **4·[BPh$_4$]** was made by the treatment of **$^{15}N_2$-3·[BPh$_4$]$_2$** with 1 equiv of base under

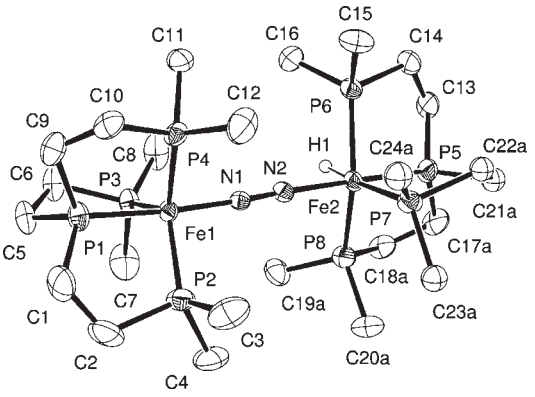

Figure 6. ORTEP plot (50% thermal ellipsoids, non-hydrogen atoms) of the complex cation of **4·[BPh$_4$]**. Disordered atoms of 20−50% occupancy and selected hydrogen atoms have been excluded for clarity.

argon. The ^{15}N NMR of **$^{15}N_2$-4·[BPh$_4$]** provides two resonances at δ −9.3 and −58.3 ppm assigned to the nitrogen bound to the iron(0) center and the iron(II), respectively, based on 2D $^{31}P-^{15}N$ HSQC NMR correlations. These assignments are supported by the ^{15}N chemical shift of **$^{15}N_2$-3·[BPh$_4$]$_2$**, reported here as δ −58.9 ppm in ethanol, and the analogous downfield ^{15}N chemical shift of the metal bound nitrogen atom of $Fe(^{15}N_2)(depe)_2$ (δ −40.5 ppm and δ −45.2 ppm unassigned)[29] relative to that of the metal bound nitrogen of $[FeH(^{15}N_2)(depe)_2]^+$ (δ −60.7 ppm Fe−N_α, and δ −42.2 ppm N_β)[17] (where depe = $Et_2PCH_2CH_2PEt_2$).

Crystals of **4·[BPh$_4$]**, suitable for analysis by X-ray crystallography, were grown by layering the THF solution with pentane, and the structure is depicted in Figure 6.

To our knowledge, this is the first crystal structure of a multivalent iron species comprising a dinitrogen bridging an iron(II) and iron(0) center. The crystal contains slight disorder within the PP_3 ligand at the iron(II) center. Selected bond lengths and angles are presented in Table 3, and crystal data in Table 4.

The iron(II) center of $[(FeH(PP_3))(\mu\text{-}N_2)(Fe(PP_3))][BPh_4]$ **4·[BPh$_4$]**, equivalent to the iron(II) centers of $[(FeH(PP_3))_2(\mu\text{-}N_2)]^{2+}$ **3·[BAr$^F_4$]$_2$**, has all Fe−P bonds slightly shorter in length than those of **3**. The bond angles are similar with notable exceptions being the N−Fe−P_T bond angles which are 92.76(5)° and 95.33(5)° in **4** compared with 90.76(7)° and 99.31(7)° in **3**. The Fe−N−N bond angle in **4** is 176.93(16)° compared with 174.7(3)° in **3**. These differences are attributed to the steric, and possibly the electronic, impact of the different second iron center. The PP_3 and dinitrogen ligands around the iron(0) center of **4** are arranged in a distorted trigonal bipyramid with a P_A−Fe−N axis. The greater than 90° P_E−Fe−N angles reflect the constraint applied to the structure by the natural bite of the PP_3 ligand. The N−N bond length of 1.127(2) Å is representative of a small degree of activation of the dinitrogen triple bond equivalent in magnitude to that observed in **3.** The N−N bond length is comparable with the N−N bond lengths of iron(0) dinitrogen complexes $Fe(N_2)(depe)_2$[30] and

(27) Smernik, R. J., Ph.D. Thesis, University of Sydney, New South Wales, Australia, 1996.
(28) Christina, H.; McFarlane, E.; McFarlane, W. *Polyhedron* **1988**, *7*, 1875–1879.
(29) Hirano, M.; Akita, M.; Morikita, T.; Kubo, H.; Fukuoka, A.; Komiya, S. *J. Chem. Soc., Dalton Trans.* **1997**, 3453–3458.
(30) Komiya, S.; Akita, M.; Yoza, A.; Kasuga, N.; Fukuoka, A.; Kai, Y. *J. Chem. Soc., Chem. Commun.* **1993**, 787–788.

Table 3. Selected Bond Distances (Å) and Angles (deg) for $[(FeH(PP_3))(\mu\text{-}N_2)(Fe(PP_3))][BPh_4]$ (**4**·[**BPh$_4$**])

Bond Distances (Å)			
Fe(1)−N(1)	1.7979(16)	Fe(2)−N(2)	1.9045(17)
Fe(1)−P(1)	2.1330(6)	Fe(2)−P(5)	2.1444(6)
Fe(1)−P(2)	2.1605(7)	Fe(2)−P(6)	2.1979(6)
Fe(1)−P(3)	2.1502(6)	Fe(2)−P(7)	2.2027(6)
Fe(1)−P(4)	2.1530(6)	Fe(2)−P(8)	2.1853(7)
N(1)−N(2)	1.127(2)	Fe(2)−H(1)	1.50(3)
Bond Angles (deg)			
Fe(1)−N(1)−N(2)	177.32(16)	Fe(2)−N(2)−N(1)	176.93(16)
N(1)−Fe(1)−P(1)	175.12(6)	N(2)−Fe(2)−P(5)	177.67(6)
P(2)−Fe(1)−P(1)	86.38(3)	P(6)−Fe(2)−P(5)	85.61(2)
P(3)−Fe(1)−P(1)	84.55(2)	P(7)−Fe(2)−P(5)	86.17(3)
P(4)−Fe(1)−P(1)	84.62(2)	P(8)−Fe(2)−P(5)	85.39(3)
N(1)−Fe(1)−P(2)	98.32(5)	N(2)−Fe(2)−P(6)	95.33(5)
P(3)−Fe(1)−P(2)	119.99(3)	P(7)−Fe(2)−P(6)	101.54(2)
P(4)−Fe(1)−P(2)	117.34(3)	P(8)−Fe(2)−P(6)	150.20(3)
N(1)−Fe(1)−P(3)	94.13(5)	N(2)−Fe(2)−P(7)	95.72(5)
P(4)−Fe(1)−P(3)	120.57(3)	P(8)−Fe(2)−P(7)	106.13(3)
N(1)−Fe(1)−P(4)	92.04(5)	N(2)−Fe(2)−P(8)	92.76(5)
N(2)−Fe(2)−H(1)	92.2(10)	P(5)−Fe(2)−H(1)	85.9(10)
P(6)−Fe(2)−H(1)	77.3(11)	P(7)−Fe(2)−H(1)	172.1(10)
P(8)−Fe(2)−H(1)	73.8(11)		

Table 4. Crystal Data Refinement Details for $[(FeH(PP_3))_2(\mu\text{-}N_2)][BAr^F{}_4]_2$ **3**·[**BAr^F$_4$**]$_2$ and $[(FeH(PP_3))(\mu\text{-}N_2)(Fe(PP_3))][BPh_4]$ **4**·[**BPh$_4$**]

	3·[**BAr^F**]$_2$	**4**·[**BPh$_4$**]
empirical formula	$C_{88}H_{86}B_2F_{48}Fe_2N_2P_8$	$C_{48}H_{81}BFe_2N_2P_8$
M	2464.67	1056.42
temp. (K)	150(2)	150(2)
crystal system	triclinic	monoclinic
space group	$P\bar{1}$	$P2_1/c$
unit cell dimensions		
a, Å	13.091(3)	15.8330(3)
b, Å	14.036(3)	17.6540(4)
c, Å	14.726(3)	19.7390(4)
α, deg	106.01(3)	
β, deg	92.18(3)	94.014(1)
γ, deg	93.96(3)	
V(Å^3)	2590.2(9)	5503.8(2)
Z	1	4
ρ(calc) (g cm^{-3})	1.580	1.275
μ(MoKα) (mm^{-1})	0.535	0.793
N	25893	155750
N_{ind}	11999	16812
N_{obs} ($I > 2\sigma(I)$)	7965	11189
$R1(F)$[a]	0.0451	0.0415
$wR2(F^2)$	0.0987	0.1030

[a] $R1 = \sum||F_o| - |F_c||/\sum|F_o|$ for $F_o > 2\sigma(F_o)$; $wR2 = [\sum w(F_o^2 - F_c^2)^2/\sum w(F_o^2)^2]^{1/2}$ all reflections $w = 1/[\sigma^2(F_o^2) + (0.03P)^2 + 0.2P]$ where $P = (F_o^2 + 2F_c^2)/3$.

$Fe(CO)_2(N_2)(PEt_3)_2$[25] at 1.14(1) and 1.08(3) Å, respectively. The trigonal bipyramidal iron complexes with tripodal phosphine ligands $[FeBr(PP^{Ph}{}_3)][BPh_4]$,[31] $[FeBr(NP^{Ph}{}_3)][PF_6]$,[31] and $Fe(CO)(NP^{iPr}{}_3)$[22] also have the monodentate ligand in an axial position *trans* to the central atom of the tetradentate ligand. Structural differences around the iron centers can be attributed to differing ligand sets and oxidation state of the iron center.

Treatment of a suspension of $[(FeH(PP_3))_2(\mu\text{-}N_2)]^{2+}$ **3**·[**BPh$_4$**]$_2$ in THF with an *excess* of potassium *tert*-butoxide under dinitrogen on a small scale in an NMR tube results in the slow dissolution of the buff colored solid to give a red solution of $[(FeH(PP_3))(\mu\text{-}N_2)(Fe(PP_3))]^+$ **4**·[**BPh$_4$**] (by $^{31}P\{^1H\}$ NMR). After a prolonged reaction time (several hours) the color of the solution fades to yellow. The $^{31}P\{^1H\}$ NMR spectrum shows the presence of two species assigned as $(Fe(PP_3))_2(\mu\text{-}N_2)$ (**5**) and $Fe(N_2)(PP_3)$ (**6**) in approximately equal amounts (Scheme 3). Complex **6** has been reported previously by the deprotonation of $[Fe(N_2)H(PP_3)]^+$ **2**·[**BPh$_4$**].[14] Each species has two $^{31}P\{^1H\}$ NMR resonances in the ratio of 1:3 corresponding to the apical phosphorus P_A and three equivalent terminal phosphorus atoms P_E of the PP_3 ligand arranged around an iron(0) center in a trigonal bipyramidal fashion. The resonance of the apical phosphorus of **6** (δ 182.9 ppm) and that of the dinitrogen bridged species **4** (δ170.9 ppm) appear as quartets because of coupling to the three equivalent P_E atoms. Correspondingly the P_E signals of **6** (δ 66.6 ppm) and **5** (δ 66.0 ppm) appear as a doublet with the coupling constant of **6** (45.8 Hz) being significantly less than that of **5** (55.7 Hz). Hence, the major effect of the second iron center on the dinitrogen ligand is to the chemical shift of the apical phosphorus located *trans* to the dinitrogen and the $^{31}P-^{31}P$ coupling across the iron(0) center.

The Fe(0) complexes $(Fe(PP_3))_2(\mu\text{-}N_2)$ **5** and $Fe(N_2)(PP_3)$ **6** were unstable and could not be isolated from solution. Attempts to crystallize the complexes by slow solvent evaporation resulted in the slow loss of the dinitrogen ligand and deposition of a dendritic iron(0) PP_3 tetramer (**7**) whose X-ray crystal structure is described in the Supporting Information.

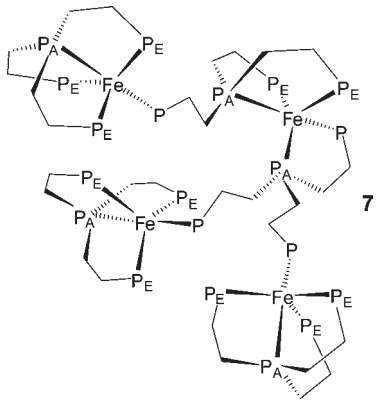

Treatment of $[(FeH(PP_3))(\mu\text{-}^{15}N_2)(Fe(PP_3))]^+$ **^{15}N$_2$-4**·[**BPh$_4$**] with potassium *t*-butoxide in deuterated benzene in an attempt to produce ^{15}N-labeled versions of complexes **5** and **6**, produced instead a mixture of $Fe(^{15}N_2)(PP_3)$ **^{15}N$_2$-6** and the C-D activation product $FeD(Ph\text{-}d_5)(PP_3)$ (**8**). In the ^{31}P NMR spectrum, the deuterated complex (**8**) exhibits multiplets at δ 176.4, 63.4, and 57.2 ppm representing P_C, P_T, and P_U, respectively with signal intensities in the ratio 1:2:1 (see Supporting Information). Each signal appears as an unresolved multiplet because of the coupling of the quadrupolar deuteride ligand in addition to the $^{31}P-^{31}P$ coupling. An authentic sample of **8** was made by the UV irradiation of $FeH_2(PP_3)$ in benzene-d_6 and the product was identical, by $^{31}P\{^1H\}$ NMR, to the product observed in the reaction of **^{15}N$_2$-4**·[**BPh$_4$**] with base in deuterated benzene. The resonance of the central phosphine P_A of $Fe(^{15}N_2)(PP_3)$ **^{15}N$_2$-6**

(31) Sacconi, L.; Di Vaira, M. *Inorg. Chem.* **1978**, *17*, 810–815.

Scheme 3

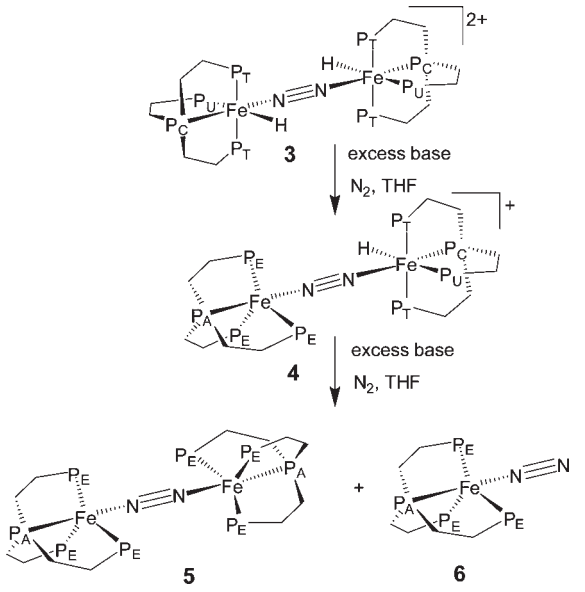

appears as a doublet of doublet of quartets at δ 182.4 ppm coupling to each nitrogen of the dinitrogen ligand and to the 3 equivalent phosphines P_E. The resonance of the terminal phosphines P_E is 3 times the intensity of the P_A signal and appears as a doublet of doublet of doublets at δ 66.4 ppm coupled to P_A and to both $^{15}N_\alpha$ and $^{15}N_\beta$ of the ^{15}N-labeled dinitrogen ligand. The coupling constants between P_A and $^{15}N_\alpha$ and $^{15}N_\beta$ are 9.5 and 1.4 Hz, respectively, and the P_E to $^{15}N_\alpha$ and $^{15}N_\beta$ coupling constants are 5.5 and 2.6 Hz, respectively. A $^{15}N\{^1H\}$ spectrum of **$^{15}N_2$-6** in THF-d_8 appears as two weak resonances for $^{15}N_\alpha$ and $^{15}N_\beta$ at δ −26.7 ppm and at δ −2.5 ppm, respectively, and these have been assigned based on their relative chemical shifts.

Under the reaction conditions described, the doubly deprotonated species $(Fe(PP_3))_2(\mu\text{-}N_2)$ **5** was not detected. The fact that the C-D activation product is observed, suggests that, in benzene-d_6 under argon, $(Fe(PP_3))_2(\mu\text{-}N_2)$ **5** is probably unstable and splits to form a reactive Fe(0) species $[Fe(PP_3)]$ and complex **6**. The $[Fe(PP_3)]$ species would react with solvent to form the observed C-D activation product (Scheme 4).

It is interesting to note that treatment of $[(FeH(PP_3))_2(\mu\text{-}N_2)]^{2+}$ **3·[BPh$_4$]$_2$** with 1 equiv of base leads cleanly to the monodeprotonated product $[(FeH(PP_3))(\mu\text{-}N_2)(Fe(PP_3))]^+$ **4·[BPh$_4$]$_2$** without any detectable formation of the doubly deprotonated product $(Fe(PP_3))_2(\mu\text{-}N_2)$ (**5**). The formation of **5** requires significantly more forcing conditions than the formation of **4**. Even though both deprotonations involve removal of a proton attached to an Fe(II) center, the second deprotonation which goes from the Fe(0)/Fe(II) (**4**) species to the Fe(0)/Fe(0) (**5**) species is much more difficult than the first which goes from the Fe(II)/Fe(II) (**3**) species to the Fe(0)/Fe(II) (**4**) species. This suggests that the influence of the electron-rich Fe(0) center in **4** is transmitted through the bridging dinitrogen.

(32) Leigh, G. J.; Jimenez-Tenorio, M. *J. Am. Chem. Soc.* **1991**, *113*, 5862–5863.

Scheme 4

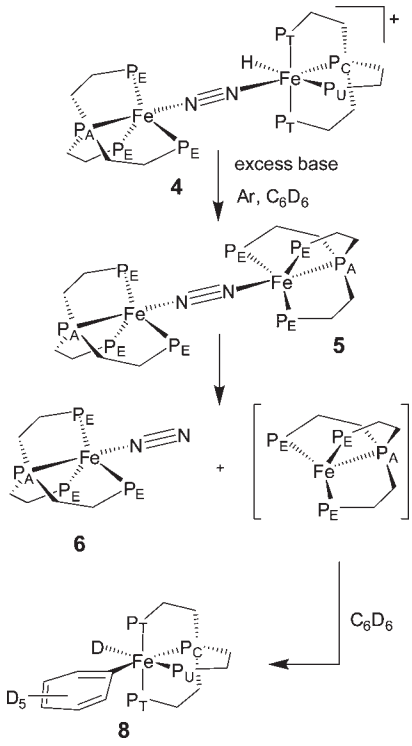

Treatment of Nitrogen Complexes with Acid. Leigh and Jimenez-Tenorio,[32] George et al.,[21] and Tyler et al.[33] have reported the formation of ammonia from related Fe(II) and Fe(0) complexes of dinitrogen when they were treated with acid. The complexes $[(FeH(PP_3))_2(\mu\text{-}N_2)]^{2+}$ **3·[BPh$_4$]$_2$**, $[Fe(PP_3)(N_2)H]^+$ **2·[BPh$_4$]**, $[(FeH(PP_3))(\mu\text{-}N_2)(Fe(PP_3))]^+$ **4·[BPh$_4$]$_2$**, $(Fe(PP_3))_2(\mu\text{-}N_2)$ **5**, and $Fe(N_2)(PP_3)$ **6** (as well as the PF_6^- and BF_4^- salts of **2**, **3**, and **4**) were each treated, on a small scale in an NMR tube with a range of acids to examine their reaction chemistry. With strong acids (HCl and HBF_4), all of the complexes were unstable and decomposed. Removal of the solvent under reduced pressure and dissolving the residue in water showed no evidence for the formation of NH_4^+ by ^{14}N NMR.[34] Treatment of $[(FeH(PP_3))(\mu\text{-}N_2)(Fe(PP_3))]^+$ **4·[BPh$_4$]$_2$**, $(Fe(PP_3))_2(\mu\text{-}N_2)$ **5**, and $Fe(N_2)(PP_3)$ **6** with a softer acid (2,6-lutidinium chloride) resulted in simple reprotonation at the Fe(0) centers to form their respective conjugate acids $[(FeH(PP_3))_2(\mu\text{-}N_2)]^{2+}$ (**3**), $[(FeH(PP_3))_2(\mu\text{-}N_2)]^{2+}$ (**3**), and $[Fe(PP_3)(N_2)H]^+$ (**2**), respectively, as the major products.

Conclusions

In this work, we have established a reasonable synthetic route to the known[14] dinuclear dinitrogen-bridged complex cation $[(FeH(PP_3))_2(\mu\text{-}N_2)]^{2+}$ (**3**), and this complex has been crystallized and structurally characterized. Successive reductive deprotonations of the two Fe(II)-H centers with base lead initially to the singly deprotonated dinitrogen bridged Fe(II)−Fe(0) species $[(FeH(PP_3))(\mu\text{-}N_2)(Fe(PP_3))]^+$ (**4**); and eventually to the doubly deprotonated dinuclear Fe(0)−Fe(0)

(33) Gilbertson, J. D.; Szymczak, N. K.; Tyler, D. R. *J. Am. Chem. Soc.* **2005**, *127*, 10184–10185.

(34) In reference experiments, it was established that NH_4^+ could be readily detected if ammonia were produced in a yield of 5%

species $(Fe(PP_3))_2(\mu\text{-}N_2)$ (**5**). The Fe(0)/Fe(II) dimer was characterized crystallographically, and to our knowledge this is the first example of a mixed valence Fe(II)/Fe(0) complex of this kind to be reported. Treatment of the reduced species (**4**) and (**5**) with mild acid reformed the parent Fe(II)−Fe(II) species (**3**) indicating that the reductive deprotonation of all of the Fe(II) hydrides to form Fe(0) species is entirely reversible and the protonation/deprotonation chemistry at the metal center still dominates the reaction chemistry of this series of dinitrogen-bridged metal complexes.

The successive deprotonation of the two Fe(II)-H centers both involve removal of a proton attached to an Fe(II) center. The first deprotonation from Fe(II)/Fe(II) species to the Fe(0)/Fe(II) species is much more facile than the second deprotonation from Fe(0)/Fe(II) to the Fe(0)/Fe(0) complex. This indicates that Fe centers are not independent, and the influence of the electron-rich Fe(0) center in $[(FeH(PP_3))(\mu\text{-})(\mu\text{-}N_2)(Fe(PP_3))]^+$ (**4**) is quite effectively transmitted through the bridging dinitrogen.

Experimental Section

General Information. All manipulations were carried out using standard Schlenk, vacuum, and glovebox techniques under a dry atmosphere of argon or nitrogen. Solvents were dried, distilled under nitrogen or argon using standard procedures,[35] and stored in glass ampules fitted with Youngs Teflon taps. THF was dried over sodium wire before distillation from sodium/benzophenone. Pentane was distilled from sodium/potassium alloy, while ethanol was distilled from diethoxymagnesium. Deuterated solvents THF-d_8 and benzene-d_6 were dried over, and distilled from, sodium/benzophenone and were vacuum distilled immediately prior to use. 2,6-Lutidinium chloride was prepared by the reaction of 2,6-lutidine with hydrogen chloride in diethyl ether. Potassium *t*-butoxide was sublimed twice prior to use. Tetrafluoroboric acid in diethyl ether (50% w/v) and 2 M hydrochloric acid in diethyl ether were degassed with three freeze−pump−thaw cycles before use. ^{15}N labeled dinitrogen was obtained from Cambridge Isotopes Laboratories and used without further purification. Air-sensitive NMR samples were prepared in an argon- or nitrogen-filled glovebox or on a high vacuum line by vacuum transfer of solvent into an NMR tube fitted with a concentric Teflon valve. ^1H and ^{15}N NMR spectra were recorded on Bruker Avance DRX400 and Bruker DPX500 NMR spectrometers operating at 400.13, 500.13 MHz (^1H) and 40.56, 50.70 MHz (^{15}N), respectively. ^{31}P NMR spectra were recorded on Bruker DPX300, Bruker Avance DRX400, and Bruker DPX500 NMR spectrometers operating at 121.49, 161.98, and 202.49 MHz, respectively. ^{14}N spectra were recorded on a Bruker Avance DRX400 at 28.92 MHz. ^2H spectra were recorded on a Bruker DPX300 at 46.07 MHz. All spectra were recorded at 300 K, unless stated otherwise. ^1H spectra were referenced to solvent resonances while ^{14}N and ^{15}N spectra were referenced to external neat nitromethane at 0.00 ppm. ^{31}P spectra were referenced to external neat trimethyl phosphite at 140.85 ppm. Microanalyses were carried out at the Campbell Microanalytical Laboratory, University of Otago, New Zealand. $FeClH(PP_3)$, $FeH_2(PP_3)$, $[(FeH(PP_3))_2(\mu\text{-}N_2)][BPh_4]_2$ (**3**·**[BPh$_4$]$_2$**), and $[Fe(N_2)H(PP_3)][BPh_4]$ (**2**·**[BPh$_4$]**) were made following literature procedures.[14,15]

$[(FeH(PP_3))_2(\mu\text{-}^{15}N_2)][BAr^F{}_4]_2$ $^{15}N_2$-3·$[BAr^F{}_4]_2$. The ^{15}N-labeled analogues of **2** and **3** were synthesized by dissolution of $FeClH(PP_3)$ (**1**) (50−100 mg, 130−260 μmol) in nitrogen-free ethanol (1 mL) in an NMR tube fitted with a concentric Teflon tap under argon. The solution was degassed by three freeze−pump−thaw cycles followed by introduction of $^{15}N_2$ to the NMR tube. **$^{15}N_2$-3:** $^{31}P\{^1H\}$ NMR (162 MHz, ethanol, benzene-d_6): δ 172.3 (1P, m, $^2J_{P(C)\text{-}N}$ = 11 Hz, **P$_C$**); 62.1 (2P, m, **P$_T$**); 59.5 (1P, m, **P$_U$**), $^1H\{^{31}P\}$ NMR (400 MHz, ethanol, benzene-d_6, high field): δ −12.9 (2H, s, Fe-**H**), $^{15}N\{^1H\}$ NMR (40.6 MHz, ethanol, benzene-d_6): δ −58.7 (2N, m) ppm. **$^{15}N_2$-2:** $^{31}P\{^1H\}$ NMR (162 MHz, ethanol/benzene-d_6): δ 171.7 (1P, m, $^2J_{P(C)\text{-}N}$ = 10 Hz, **P$_C$**); 62.9 (2P, m, **P$_T$**); 61.0 (1P, m, **P$_U$**) ppm; $^1H\{^{31}P\}$ NMR (400 MHz, ethanol/benzene-d_6, high field): δ −13.1 (2H, s, Fe-**H**), $^{15}N\{^1H\}$ NMR (40.6 MHz, ethanol, benzene-d_6): δ −34.2 (1N, br s, Fe−N**N**); −63.4 (1N, m, Fe-**N**) (lit.[17] −35.0 Fe−N**N**, −63.7 Fe-**N**). Crystals of **$^{15}N_2$-3·$[BAr^F{}_4]_2$** suitable for X-ray diffraction were grown by addition of sodium tetra(3,5-bis-(trifluoromethyl)phenyl)borate (100 mg, 11 mmol) to the ethanol solution of **$^{15}N_2$-3** and **$^{15}N_2$-2**. Pale orange crystals of **$^{15}N_2$-3·$[BAr^F{}_4]_2$** formed after leaving the solution to stand under an atmosphere of argon for several weeks.

$[(FeH(PP_3))(\mu\text{-}N_2)(Fe(PP_3))][BPh_4]$ 4·[BPh$_4$]. Potassium *t*-butoxide (8 mg, 71 μmol) was added to a suspension of $[(FeH(PP_3))_2(\mu\text{-}N_2)][BPh_4]_2$ **3·[BPh$_4$]$_2$** (96 mg, 70 μmol) in THF (approximately 4 mL). The reaction mixture was stirred with gentle heating (approximately 50 °C) for 2 h after which time the solution had a red color and had precipitated a white solid. The solution was filtered and layered with pentane and $[(FeH(PP_3))(\mu\text{-}N_2)(Fe(PP_3))][BPh_4]$ deposited as a red crystalline solid (15 mg, 21%) suitable for analysis by X-ray diffraction. An identical product was isolated when the base used in this reaction was potassium bis(trimethylsilyl)amide. Anal. Found: C 54.34, H 7.91, N 2.49. $C_{48}H_{81}BFe_2N_2P_8$ (MW 1056.46) requires C 54.57, H 7.73, N 2.65. $^{31}P\{^1H\}$ NMR (162 MHz, THF-d_8): δ 180.7 (1P, ddtq, $^2J_{P(A)\text{-}P(E)}$ = 46.7 Hz, $^5J_{P(A)\text{-}P(U)}$ = 2.2 Hz, $^2J_{P(A)\text{-}P(T)}$ = 2.0 Hz, $^2J_{P(A)\text{-}P(C)}$ = 0.85 Hz, **P$_A$**); 176.7 (1P, ddtq, $^2J_{P(C)\text{-}P(T)}$ = 29.7 Hz, $^2J_{P(C)\text{-}P(U)}$ = 22.4 Hz, $^2J_{P(C)\text{-}P(E)}$ = 0.90 Hz, **P$_C$**); 67.0 (3P, dddt, $^2J_{P(E)\text{-}P(U)}$ = 5.3 Hz, $^2J_{P(E)\text{-}P(T)}$ = 4.5 Hz, **P$_E$**); 62.0 (2P, dddq, $^2J_{P(T)\text{-}P(U)}$ = 18.0 Hz, **P$_T$**); 59.6 (1P, ddtq, **P$_U$**) ppm. $^1H\{^{31}P\}$ NMR (400 MHz, THF-d_8, selected resonances): δ 1.64 (6H, s, 2 × P_T-C**H**$_3$); 1.46 (6H, s, 2 × P_U-C**H**$_3$); 1.45 (6H, s, 2 × P_T-C**H**$_3$); 1.36 (18H, s, 6 × P_E-C**H**$_3$); −12.5 (1H, br s, Fe-**H**) ppm.

$[(FeH(PP_3))(\mu\text{-}^{15}N_2)(Fe(PP_3))][BPh_4]$ $^{15}N_2$-4·[BPh$_4$]. The ^{15}N-labeled analogue of **4** was synthesized by treatment of $[(FeH(PP_3))_2(\mu\text{-}^{15}N_2)][BAr^F{}_4]_2$ **$^{15}N_2$-3·$[BAr^F{}_4]_2$** (100 mg, 85 μmol) in THF-d_8 (0.7 mL) with potassium *t*-butoxide (4.5 mg, 40 μmol) under argon. The reaction mixture was heated to approximately 60 °C for an hour in an NMR tube fitted with a concentric Teflon valve. The resulting dark red solution of **$^{15}N_2$-3·[BPh$_4$]** was filtered prior to analysis by NMR spectroscopy. $^{31}P\{^1H\}$ NMR (202 MHz, THF-d_8): δ 180.6 (1P, m, $^2J_{P(A)\text{-}N}$ = 10 Hz, **P$_A$**); 176.6 (1P, m, **P$_C$**); 66.9 (3P, m, **P$_E$**); 61.9 (2P, m, **P$_T$**); 59.5 (1P, m, **P$_U$**) ppm. $^1H\{^{31}P\}$ NMR (500 MHz, THF-d_8, high field): δ −12.6 (1H, m, Fe-**H**) ppm. $^{15}N\{^1H\}$ NMR (50.7 MHz, THF-d_8): δ −9.3 (1N, s, P_A-Fe-**N**), −58.3 (1N, s, P_C-Fe-**N**) ppm.

Reaction of $[(FeH(PP_3))_2(\mu\text{-}N_2)][BPh_4]_2$ (3·[BPh$_4$]$_2$) with Excess Base. (3·[BPh$_4$]$_2$) (95 mg, 70 μmol) was placed in an NMR tube under dinitrogen in THF (0.5 mL) and shaken to form a slurry. To this an excess of potassium *t*-butoxide was added (30 mg, 270 μmol). The buff colored solid slowly dissolved to give a red solution (shown by $^{31}P\{^1H\}$ NMR to be $[(FeH(PP_3))(\mu\text{-}N_2)(Fe(PP_3))][BPh_4]$ **4·[BPh$_4$]** after 24 h). The color of the solution slowly changed to yellow solution and after 3 days the solution was shown by $^{31}P\{^1H\}$ NMR to contain two major species, namely, $(Fe(PP_3))_2(\mu\text{-}N_2)$ (**5**) and $Fe(N_2)(PP_3)$ (**6**). $(Fe(PP_3))_2(\mu\text{-}N_2)$ (**5**): $^{31}P\{^1H\}$ NMR (121.5 MHz, THF): δ 170.9 (1P, q, **P$_A$**, $^2J_{P(A)\text{-}P(E)}$ = 57.7 Hz); 66.0 (3P, d, **P$_E$**) ppm. $Fe(N_2)(PP_3)$ (**6**): $^{31}P\{^1H\}$ NMR (121.5 MHz, THF): δ 182.9 (1P, q, **P$_A$**, $^2J_{P(A)\text{-}P(E)}$ = 45.3 Hz); 66.6 (3P, d, **P$_E$**) (lit.[14] 181.7 **P$_A$**, 66.0 **P$_E$**) ppm.

Reaction of $[(FeH(PP_3))(\mu\text{-}^{15}N_2)(Fe(PP_3))][BPh_4]$ ($^{15}N_2$-4·[BPh$_4$]) with base. $Fe(^{15}N_2)(PP_3)$ **$^{15}N_2$-6** was synthesized by treatment of an NMR sample of **$^{15}N_2$-4·[BPh$_4$]** (24 mg, 10 μmol) with potassium *t*-butoxide (1 mg, 10 μmol) in benzene-d_6 (0.5 mL) at room temperature. This reaction resulted in two major products.

(35) Perrin, D. D. A.; Perrin, W. L. F. *Purification of Laboratory Chemicals*., 3rd ed.; Pergamon Press: Oxford, 1993.

The first assigned as Fe($^{15}N_2$)(PP_3) **$^{15}N_2$-6**, the second was assigned as the C-D activation product FeD(Ph-d_5)(PP_3) **8**. **$^{15}N_2$-6**: $^{31}P\{^1H\}$ NMR (202.5 MHz, benzene-d_6): δ 182.4 (1P, ddq, $^2J_{P(A)\text{-}P(E)}$ = 45.4 Hz, $^2J_{P(A)\text{-}N}$ = 9.5 Hz, $^3J_{P(A)\text{-}N}$ = 1.4 Hz, $\mathbf{P_A}$); 66.4 (3P, ddd, $^2J_{P(E)\text{-}N}$ = 5.5 Hz, $^3J_{P(E)\text{-}N}$ = 2.6 Hz, $\mathbf{P_E}$) ppm. **8**: $^{31}P\{^1H\}$ NMR (202.5 MHz, benzene-d_6): δ 176.4 (1P, m, $\mathbf{P_C}$); 63.4 (2P, m, $\mathbf{P_T}$), 57.2 (1P, m, $\mathbf{P_U}$) ppm.

FeD(Ph-d_5)(PP_3) 8. An authentic sample of FeD(Ph-d_5)(PP_3) **8** was prepared by irradiating a solution of $FeH_2(PP_3)$ in benzene-d_6. A solution of $FeH_2(PP_3)$ (10 mg) in benzene-d_6 was irradiated for 1 h at room temperature using a 300 W mercury UV lamp source. $^{31}P\{^1H\}$, ^2H and ^1H NMR indicated the complete consumption of the starting material and the formation of FeD(Ph-d_5)(PP_3) **6** as the only product. $^{31}P\{^1H\}$ NMR (121.5 MHz, benzene-d_6): δ 176.4 (1P, m, $\mathbf{P_C}$); 63.7 (2P, m, $\mathbf{P_T}$); 57.4 (2P, m, $\mathbf{P_U}$). ^2H NMR (46.1 MHz, benzene-d_6): δ −15.1 (1D, m, Fe-**D**) ppm. The unique pattern of coupling constants, splitting patterns, and chemical shifts were consistent with the product formed from the base treatment of [(FeH(PP_3))(μ-$^{15}N_2$)(Fe(PP_3))][BPh_4] **$^{15}N_2$-4·[BPh_4]** previously described.

Treatment of Iron Dinitrogen Complexes with Acid. In a typical reaction, 30−60 mg of [(FeH(PP_3))$_2$(μ-N_2)][BPh_4]$_2$ **3·[BPh_4]$_2$** (20−40 μmol) was placed in an NMR tube under dinitrogen or argon, and HCl (0.5 mL, 2 M, 500 μmol) in diethyl ether was added. The reaction was immediate, and bubbles were evolved with the formation of both a white and a red solid. The reaction mixture was either shaken ensuring immediate access of the acid to all dinitrogen salt or left undisturbed to allow the reaction to proceed more slowly over the course of several hours. Reaction progress was monitored by $^{31}P\{^1H\}$ NMR. To test whether NH_4^+ was produced during the reaction, the solvent was removed under reduced pressure, and the solid residue was dissolved in water containing one drop of D_2O for NMR lock. ^{14}N NMR was used to detect the presence of NH_4^+ (around −360 ppm). A similar procedure was also performed on [Fe(PP_3)(N_2)H]$^+$ **2·[BPh_4]**, **3·[BF_4]$_2$**, **3·[PF_6]$_2$** and with the alternative acids tetrafluoroboric acid and 2,6-lutidinium chloride.

Treatment of Iron Dinitrogen Complexes with Base Then Acid. In a typical reaction, 30−85 mg of [(FeH(PP_3))$_2$(μ-N_2)][BPh_4]$_2$ **3·[BPh_4]$_2$** (20−55 μmol) was placed in an NMR tube with 1 mL of THF under dinitrogen or argon and an excess of potassium *t*-butoxide added (200−300 μmol). The NMR tube was heated gently until a deep red [(FeH(PP_3))(μ-N_2)(Fe(PP_3))][BPh_4] **4·[BPh_4]** or yellow mixture of (Fe(PP_3))$_2$(μ-N_2) **5** and Fe(N_2)(PP_3) **6** was formed. The solution was filtered and then treated, with an excess of acid (approximately 0.5−1 mL 2 M HCl in diethyl ether) causing effervescence and the immediate formation of both a white and a red solid. The reaction mixture was either shaken ensuring immediate access of the acid to all dinitrogen complex or left undisturbed to allow the reaction to proceed more slowly over the course of several hours. Reaction progress was monitored by $^{31}P\{^1H\}$ NMR. To test whether NH_4^+ was produced during the reaction, the solvent was removed under reduced pressure, and the solid residue was dissolved in water containing one drop of D_2O for NMR lock. ^{14}N NMR was used to detect the presence of NH_4^+ (around −360 ppm).

Acknowledgment. The authors thank the Australian Research Council for financial support. We also thank Dr. Susanne L. Huth, Dr. Marcia Scudder, and Dr. Paul Jensen from the University of Sydney for assistance with the crystal structures.

Supporting Information Available: A CIF file with crystallographic data for compounds [(FeH(PP_3))$_2$(μ-N_2)][$BAr^F{}_4$]$_2$ **3·[$BAr^F{}_4$]$_2$**, [(FeH(PP_3))(μ-N_2)(Fe(PP_3))][BPh_4] **4·[BPh_4]**, and the dendritic iron(0) PP_3 tetramer **7**; a pdf file containing a structural description for a dendritic iron(0) PP_3 tetramer (**7**) and ^{31}P NMR spectral data for FeD(Ph-d_5)(PP_3) **8**. This material is available free of charge via the Internet at http://pubs.acs.org.